Feasibility of Simultaneous Stress ^{99m}Tc-Sestamibi/Rest ^{201}Tl Dual-Isotope Myocardial Perfusion SPECT in the Detection of Coronary Artery Disease

Mashio Nakamura, Kan Takeda, Takashi Ichihara, Nobutoku Motomura, Hiroyuki Shimizu, Yasuhiro Saito, Yoshiyuki Nomura, Naoki Isaka, Tokuji Konishi and Takeshi Nakano

First Department of Internal Medicine and Department of Radiology, Mie University, Tsu, and Toshiba Nasu Works, Otawara, Japan

This study assesses feasibility and diagnostic accuracy of simultaneous stress ^{99m}Tc-sestamibi/rest ^{201}Tl dual-isotope myocardial perfusion SPECT with Moore's correction method, in which contamination originating from lead x-rays produced in a collimator was subtracted in the ^{201}Tl windows. **Methods:** Eighty-one patients with suspected coronary artery disease received exercise ^{99m}Tc-sestamibi injection, followed by rest ^{201}Tl injection 50 min later, and dual-isotope SPECT was performed (group 1). These results were compared with coronary angiographic findings. Furthermore, to estimate the accuracy of Moore's correction method, ^{201}Tl crosstalk into the ^{99m}Tc acquisition window (group 2A, n = 20) and ^{99m}Tc crosstalk into the ^{201}Tl acquisition windows (group 2B, n = 20) were studied. For group 2A, stress ^{99m}Tc-sestamibi SPECT (single ^{99m}Tc-sestamibi SPECT) was performed, followed by ^{201}Tl injection at rest and dual-isotope SPECT acquisition 50 min later. For group 2B, rest ^{201}Tl SPECT (single ^{201}Tl SPECT) was performed, followed by ^{99m}Tc-sestamibi injection at rest and dual-isotope SPECT acquisition 30 min later. **Results:** Sensitivity and specificity in group 1 were 83% and 99%, respectively, when ≥75% coronary artery narrowing was considered significant. In groups 2A and 2B, SPECT images were divided into 24 segments, and relative regional uptake in each segment was obtained. In group 2A, relative regional uptake of single ^{99m}Tc-sestamibi SPECT correlated well with that of dual-isotope SPECT (r = 0.942). In group 2B, relative regional uptake of single ^{201}Tl SPECT correlated well with that of dual-isotope SPECT (r = 0.935). Furthermore, in low ^{201}Tl uptake segments with relative regional uptake in both single- and dual-isotope SPECT of ≤70%, the degree of concordance between single- and dual-rest ^{201}Tl was considered to be high with Bland-Altman analysis and the kappa statistic. Comparison of perfusion defect type demonstrated that, of 22 stress defects within infarct zones, 95% were irreversible and 5% were reversible. In contrast, of 28 stress defects within stenosed vessel zones in noninfarct zones, 89% were reversible and 11% were irreversible ($P < 0.0001$ versus infarct zones). **Conclusion:** Simultaneous dual-isotope imaging with Moore's correction method is feasible, with acceptable accuracy for detection of coronary artery disease and a small amount of crosstalk into each window.

Received Apr. 8, 1998; revision accepted Jan. 12, 1999.

For correspondence or reprints contact: Mashio Nakamura, MD, First Department of Internal Medicine, Mie University, Edobashi 2–174, Tsu 514, Japan.

Key Words: SPECT; ^{99m}Tc-sestamibi; dual-isotope imaging; ^{201}Tl

J Nucl Med 1999; 40:895–903

Because standard gamma cameras now have the ability to distinguish radioisotopes of differing energy, dual-isotope myocardial SPECT with separate acquisition of rest ^{201}Tl and stress ^{99m}Tc-sestamibi for the assessment of myocardial perfusion has been developed (*1–4*). Although this separate acquisition approach eliminates the delay between rest and stress studies and provides rest ^{201}Tl images that are uncontaminated by the higher energy photons of ^{99m}Tc, there are several advantages in performing simultaneous ^{99m}Tc/^{201}Tl dual-isotope SPECT imaging, which requires only one data acquisition and therefore halves the camera time, significantly abbreviating the length of the overall study and permitting ^{201}Tl and ^{99m}Tc data to be acquired during the same camera orbit under identical conditions of patient motion, positioning and attenuation paths. However, if the ^{201}Tl images were obtained after injection of the ^{99m}Tc agent, the ^{201}Tl low-energy window would be contaminated, mostly by scattered ^{99m}Tc photons, due to the relatively high activity of injected ^{99m}Tc compared with that of ^{201}Tl. Therefore, for this technique to be clinically applicable, a reliable correction method for the crosstalk of ^{99m}Tc into the ^{201}Tl windows must be established.

In 1995, Moore et al. (*5*) performed a simulation study and concluded that a new correction method for the crosstalk of ^{99m}Tc into the ^{201}Tl windows must be established. They reported that contamination originating from lead x-rays produced in the collimator had to be subtracted in the ^{201}Tl windows.

This study was undertaken to assess the feasibility of simultaneous stress ^{99m}Tc-sestamibi/rest ^{201}Tl dual-isotope myocardial perfusion SPECT using Moore's correction method and the accuracy of Moore's correction method in clinical studies.

MATERIALS AND METHODS

Patient Population

Eighty-one patients (group 1: 65 men, 16 women; mean age 65 ± 9 y) with suspected coronary artery disease (CAD), who were clinically referred for stress myocardial perfusion scintigraphy, underwent simultaneous stress ^{99m}Tc-sestamibi/rest ^{201}Tl dual-isotope myocardial perfusion SPECT. All patients underwent coronary angiography using standard techniques within 2 wk of each other. The results of the coronary angiograms were interpreted by three angiographers who were blinded to the results of perfusion imaging. The presence of CAD was defined as ≥75% diameter stenosis in one or more of the main coronary arteries or their major branches. Twenty-two patients in group 1 previously had myocardial infarction, defined by a documented history of myocardial infarction or the presence of Q waves on electrocardiography and the demonstration of akinetic or dyskinetic myocardial regions on left ventriculography or rest echocardiography.

To assess the accuracy of Moore's correction method, we examined two other groups. In 20 patients with suspected CAD (group 2A: mean age 62 ± 7 y), ^{201}Tl crosstalk into the ^{99m}Tc acquisition window was estimated. In a separate population of 20 patients with suspected CAD (group 2B: mean age 63 ± 7 y), ^{99m}Tc crosstalk into the ^{201}Tl acquisition windows was estimated.

Protocol Design

Patients in group 1 first received ^{99m}Tc-sestamibi injection (740 MBq [20 mCi]) at peak exercise, followed by rest ^{201}Tl injection (111 MBq [3 mCi]) 50 min later, and SPECT acquisition was then performed 5 min later using dual-isotope (^{99m}Tc plus ^{201}Tl) energy windows (Fig. 1). (Simultaneously acquired stress ^{99m}Tc-sestamibi and rest ^{201}Tl SPECT are referred to hereinafter as dual-stress ^{99m}Tc-sestamibi and dual-rest ^{201}Tl.)

Patients in group 2A received ^{99m}Tc-sestamibi injection (740 MBq [20 mCi]) at peak stress, followed by SPECT imaging 15 min later. ^{201}Tl (111 MBq [3 mCi]) was injected 50 min after ^{99m}Tc-sestamibi injection, and SPECT acquisition was then performed 5 min later using dual-isotope windows (Fig. 2A). For patients in group 2B, rest SPECT after ^{201}Tl injection (111 MBq [3 mCi]) was performed first. ^{99m}Tc-sestamibi (740 MBq [20 mCi]) was then injected at rest, and SPECT acquisition was performed 30 min later using dual-isotope windows (Fig. 2B). (Stress ^{99m}Tc-sestamibi studies acquired before rest ^{201}Tl injection and therefore uncontaminated by ^{201}Tl crosstalk are referred to hereinafter as single-stress ^{99m}Tc-sestamibi. Rest ^{201}Tl studies acquired before rest ^{99m}Tc-sestamibi injection and therefore uncontaminated by ^{99m}Tc-sestamibi crosstalk are referred to hereinafter as single-rest ^{201}Tl.)

Exercise Testing

Symptom-limited exercise testing was performed on an ergometer, starting at a 50-W workload, with a 25-W increase every 3 min. Exercise was terminated if one or more of the following occurred: angina of at least moderate degree, excessive fatigue, weakness, shortness of breath, ≥2 mm ST segment depression or dizziness. At the end of exercise, ^{99m}Tc-sestamibi was injected, and patients were exercised for 1 additional minute.

SPECT Acquisition with Moore's Correction Method and Processing Protocols

SPECT was performed with a three-head, rotating camera, dedicated SPECT system (GCS-9300A/DI; Toshiba Medical Systems, Tokyo, Japan), equipped with a low-energy, high-resolution collimator. A total of 60 projection images with a 64 × 64 matrix were obtained over 360° at 30 s per projection.

The energy windows selected for dual-isotope (^{99m}Tc plus ^{201}Tl) SPECT using Moore's correction method were as follows: (A) 62–84 keV, (B) 90–110 keV, (C) 129.5–150.5 keV and (D) 157–183 keV (Fig. 3). Moore et al. (*6*) used a Monte Carlo program, which simulates all details of photon transport, to demonstrate that lead radiographs produced in a collimator by photons with energy ≥88 keV may contribute significantly to the total contamination in window A. They also observed that the spatial distribution of the multiply scattered ^{99m}Tc photons detected in window A differed from that of the lead radiographs and that the point-spread function of lead radiographs was more strongly dominated by the primary ^{99m}Tc photopeak. Therefore, they attempted to estimate each projection image of the contamination in window A as a linear combination of the image in a scatter-window B, I_B, blurred by a two-dimensional radial Gaussian smoothing filter, G_B, and the ^{99m}Tc photopeak image in window C, I_C, blurred by a different filter, G_C:

$$I_A,\text{contam.} = k_B(I_B ** G_B) + k_C(I_C ** G_C).$$

$$\text{Tl(single)} = I_A - I_A,\text{contam.} \qquad \text{Eq. 1}$$

In equation 1, the operator, **, refers to a two-dimensional convolution. The ^{99m}Tc image was corrected by

$$I_C,\text{contam.} = k_D I_D$$

$$^{99m}\text{Tc (single)} = I_C - I_C,\text{contam.} \qquad \text{Eq. 2}$$

The constants k_B, k_C, k_D, G_B and G_C were determined by analyzing projection data simulated for the mathematical phantom (*5*).

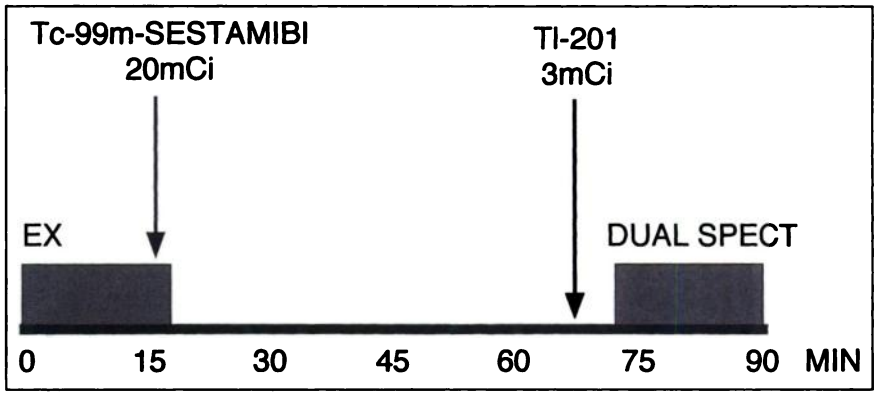

FIGURE 1. Schematic outline of exercise and imaging protocols used for group 1. EX = exercise.

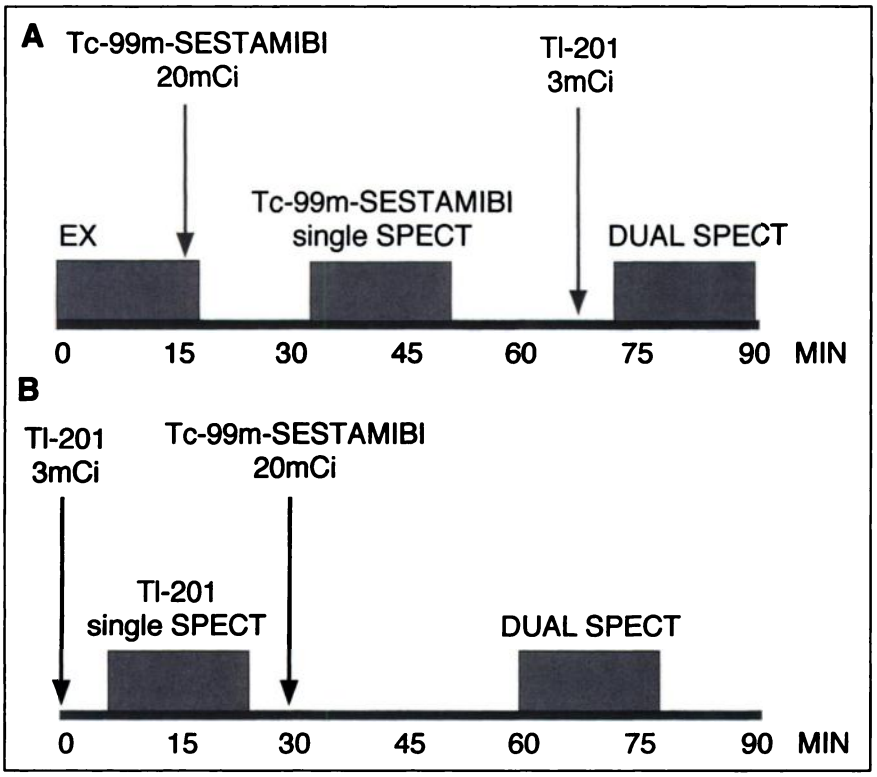

FIGURE 2. Schematic outline of exercise and imaging protocols using ^{99m}Tc-sestamibi (A) and ^{201}Tl (B) for group 2. EX = exercise.

For our collimator, we determined the factors k_B, k_C, k_D, G_B and G_C in our phantom study. A thorax phantom (Model ECT/LUNG/P; Data Spectrum Corp., Hillsborough, NC) containing a cardiac insert and a fluorocarbon-coated nonstick rod to simulate the spine was used. To determine the factors k_B, k_C, G_B and G_C, the phantom was filled with ^{99m}Tc alone. To determine the factor k_D, the phantom was filled with ^{201}Tl alone. The values of k_B, k_C and k_D were 1.38, 0.18 and 0.67, respectively. G_B and G_C were the same Butterworth filter, of which conditions were order 8 and cutoff frequency 0.34 cycle/cm.

For single-stress ^{99m}Tc-sestamibi SPECT (group 2A), a 15% symmetric window centered on the 140-keV photopeak was used. For single-rest ^{201}Tl SPECT (group 2B), a 20% symmetric window centered on the 68- to 80-keV photopeak and a 10% window centered on the 167-keV photopeak were used.

Projection images were filtered with a Butterworth filter before reconstruction. Image reconstruction was based on filtered backprojection with a ramp filter and produced transverse tomograms of 6.4-mm axial thickness, encompassing the entire heart. Sagittal and oblique tomograms parallel to the long and short axes of the left

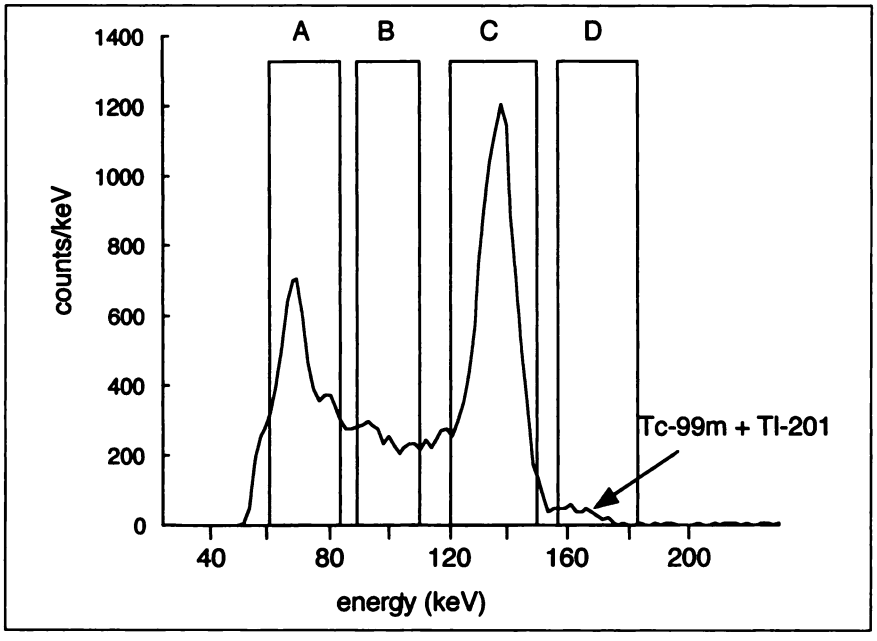

FIGURE 3. Energy spectra of simultaneous dual-isotope imaging with Moore's correction method. Energy windows were 62–84 (A), 90–110 (B), 129.5–150.5 (C) and 157–183 keV (D).

ventricle were extracted from the transaxial tomograms by performing a coordinate transformation with appropriate interpolation. In the dual-isotope data, the same rotation angles were used for both stress and rest data. Attenuation or scatter correction was not applied.

Visual Dual-Isotope SPECT Analysis

The distribution of dual-stress ^{99m}Tc-sestamibi and dual-rest ^{201}Tl uptake in group 1 was analyzed qualitatively in the three standard orthogonal tomographic imaging planes as follows: the septal, apical and lateral regions in the horizontal long-axis view; the anterior, apical and inferior regions in the vertical long-axis view; and the anterior, septal, inferior and lateral regions in the short-axis view. The intensity of each image was normalized to the highest pixel value in that image. Separate images were obtained displaying aligned slices of the dual-stress ^{99m}Tc-sestamibi with the corresponding dual-rest ^{201}Tl SPECT. The images were graded by two experienced, blinded observers on a 5-point scale from 0, markedly reduced/absent activity, to 2, definitely reduced, to 4, normal. Differences were resolved by consensus. The grade assigned to a given region was the lowest regional score from all tomographic slices and views. A stress defect was defined as a region on the dual-stress ^{99m}Tc-sestamibi SPECT with a score of $\leq$2. A region was determined to be irreversible if the assigned regional grade was abnormal and it remained at the same abnormal grade on subsequent images. Similarly, a region was determined to be reversible if the assigned abnormal regional grade increased or normalized on subsequent images. When the imaging results were analyzed with respect to coronary artery anatomy, the segments were assigned anatomic regions as follows: left anterior descending artery: anterior, apical and septal regions; left circumflex artery: lateral region; and right coronary artery: inferior region. For each image, the three major vascular territories were categorized as normal or abnormal. An abnormal vascular territory was defined as having at least one stress defect. Abnormal territories were then subcategorized as reversible defects or irreversible defects. In regions in which both reversible and irreversible defects were observed in the same vascular territory, the region was considered reversible in this analysis. Myocardial infarct zones were defined as tomographic segments within the vascular territories of the infarcted vessels.

Quantitative Assessment of the Accuracy of Moore's Correction Method

The accuracy of Moore's correction method was evaluated by comparison of the relative regional uptake between dual SPECT and the corresponding single SPECT in group 2A and group 2B. Myocardial polar maps constructed from raw maximal-count circumferencial profiles of short-axis slices were created for each dual/single pair and normalized to the maximum count within each map. Myocardial polar maps were divided into 24 segments. Then, the relative regional uptake in each segment of the myocardial polar maps was calculated.

Statistical Methods

All continuous variables are reported as mean $\pm$ SD. The mean differences for continuous variables were compared using the paired Student t test. Comparison of proportion between perfusion defect type in infarct and noninfarct zones was computed with a chi-square statistic or, when appropriate, with the Fisher exact test. Linear regression, Bland-Altman analysis and the kappa statistic were performed to evaluate the correlation of the relative regional uptake between dual SPECT and the corresponding single SPECT. In the kappa statistic, a value of 1 denotes perfect agreement, and 0 indicates no agreement beyond chance; values $\geq$ 0.6 are considered indicative of good agreement. A two-tailed P value < 0.05 was considered to represent statistical significance.

RESULTS

Sensitivity, Specificity and Accuracy of Visual Dual-Isotope SPECT Analysis for Detection of Coronary Artery Disease (Group 1)

With $\geq$75% narrowing of the coronary artery considered significant, the sensitivity, specificity and accuracy for overall detection of diseased vessels using dual-isotope SPECT in group 1 were 83% (50/60 territories), 99% (182/183 territories) and 95% (232/243 territories), respectively (Table 1). Excluding myocardial infarct zones, the sensitivity, specificity and accuracy of dual-isotope SPECT for disease detection were 74% (28/38 territories), 99% (182/183 territories) and 95% (210/221 territories), respectively, with $\geq$75% narrowing considered significant. The patients with CAD who had false-negative results by SPECT tended to have mild stenosis (50%–70%) or branch lesions.

Perfusion Defect Type in Infarct and Noninfarct Zones (Group 1)

There were 22 territories with stress defects in infarct zones in group 1. Of these, 21 territories (95%) were irreversible, and 1 territory (5%) was reversible (Fig. 4). In contrast, among 28 territories with stress defects within the stenosed vessel zones in the noninfarct zones in group 1, 25 territories (89%) had reversible defects, and 3 territories (11%) had irreversible defects ($P < 0.0001$ versus infarct zone in the Fisher exact test).

Case Example in Group 1

Figure 5 shows a typical example of a reversible defect in a simultaneous acquisition dual-isotope SPECT study of a 67-y-old man with typical angina and no previous myocardial infarction. The stress ^{99m}Tc-sestamibi images showed severe defects in the territory of the left anterior descending coronary artery, and the rest ^{201}Tl images were normal. Subsequent catheterization revealed a 90% stenosis of the left anterior descending coronary artery and no other significant abnormalities.

TABLE 1
Sensitivity, Specificity and Accuracy of Dual-Isotope SPECT for Detection of Coronary Artery Disease (CAD)

	Sensitivity	Specificity	Accuracy
Overall CAD	83% (50/60)	99% (182/183)	95% (232/243)
CAD without prior MI	74% (28/38)	99% (182/183)	95% (210/221)

MI = myocardial infarction.

	NR	REV
MI ZONE	21	1
NON-MI ZONE	3	25

FIGURE 4. Comparison of perfusion defect type in dual-isotope SPECT between myocardial infarction (MI) zone versus non-MI zone. MI zone versus non-MI zone, $P < 0.0001$ by Fisher exact test. NR = nonreversible; REV = reversible.

Quantitative Assessment of the Accuracy of Moore's Correction Method

Comparison Between Dual- and Single-Stress ^{99m}Tc-Sestamibi SPECT (Group 2A). The relative regional uptake was compared between single-stress ^{99m}Tc-sestamibi and dual-stress ^{99m}Tc-sestamibi SPECT in 480 SPECT segments. The plot is shown in Figure 6A, which reveals a strong linear relationship between the relative regional uptake of single- and dual-stress ^{99m}Tc-sestamibi SPECT, with a regression equation close to the identical line ($y = 0.97x + 1.6$, $r = 0.942$, $P < 0.0001$) and a small 95% confidence interval for the mean value of estimated dual-stress ^{99m}Tc-sestamibi SPECT. In addition, the relative regional uptake values of single- and dual-stress ^{99m}Tc-sestamibi SPECT were 76% ± 15% and 77% ± 15%, respectively. There was no difference in the mean relative regional uptake between single- and dual-stress ^{99m}Tc-sestamibi SPECT. Therefore, a high degree of concordance was recognized between single- and dual-stress ^{99m}Tc-sestamibi.

Comparison Between Dual- and Single-Rest ^{201}Tl (Group 2B). The plot for the relative regional uptake is shown in Figure 6B. The plot shows a strong linear relationship between single- and dual-rest ^{201}Tl SPECT in 480 SPECT segments, with a regression equation close to the identical line ($y = 0.95x + 4.5$, $r = 0.937$, $P < 0.0001$) and a small 95% confidence interval for the mean value of estimated dual-rest ^{201}Tl SPECT. In addition, the relative regional uptake values of single- and dual-rest ^{201}Tl were 76% ± 15% and 75% ± 16%, respectively. There was no difference in the mean relative regional uptake between single- and dual-rest ^{201}Tl SPECT. Furthermore, in the segments with relative regional uptake values in both single- and dual-rest ^{201}Tl of ≤70%, additional analyses were performed because the correction for the crosstalk of ^{99m}Tc into the ^{201}Tl windows in the low-uptake region seemed to be the most important point at issue. The result of linear regression in the regional uptake of dual-rest ^{201}Tl SPECT on single-rest ^{201}Tl SPECT is shown in Figure 7. The plot shows a strong linear relationship between single- and dual-rest ^{201}Tl SPECT in 154 low-uptake SPECT segments, with a regression equation close to the identical line ($y = 0.92x + 4.3$, $r = 0.839$, $P < 0.0001$) and a small 95% confidence interval for the mean value of estimated dual-rest ^{201}Tl SPECT. Figure 8 shows the plot of the difference in the relative regional uptake values between single- and dual-rest ^{201}Tl SPECT against their mean, using Bland-Altman analysis. The difference was not significant, the positive bias was small (0.4%) and the 95% confidence intervals for the difference were narrow (−12.2% to 11.8%). Because comparison of the relative regional uptake values showed agreement between single- and dual-rest ^{201}Tl SPECT with the kappa statistic, the relative regional uptake values in the range of 21%–70% were divided into five ranks at intervals of 10%. The concordance in each group of the relative regional uptake between

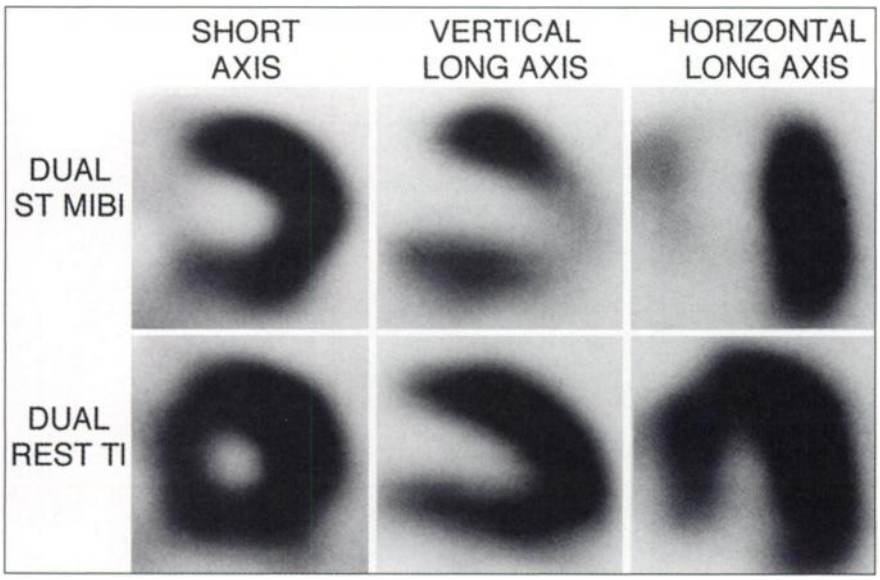

FIGURE 5. Example of dual-isotope study in group 1 patient (67-y-old man) with reversible perfusion defect. ST MIBI = stress ^{99m}Tc sestamibi; Tl = ^{201}Tl.

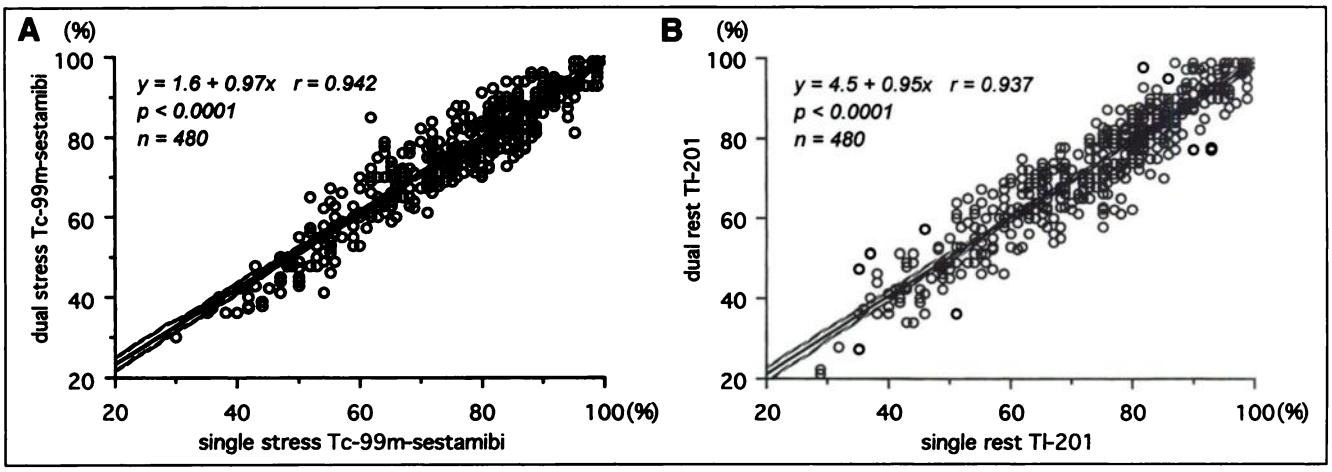

FIGURE 6. Correlation between relative regional uptake of ^{99m}Tc-sestamibi (A) and ^{201}Tl (B) obtained by single SPECT and by dual SPECT. Solid line represents regression line. Dotted curves represent 95% confidence interval for mean value of estimated dual-isotope SPECT (^{99m}Tc-sestamibi; $y = 4.5 + 0.95x \pm 0.03\sqrt{225 + [x - 7.65]^2}$ ^{201}Tl; $y = 1.7 + 0.97x \pm 0.1\sqrt{251.2 + [x - 74.1]^2}$).

single- and dual-rest ^{201}Tl SPECT (Fig. 9) was 60.4% (κ = 0.67). Thus, the degree of concordance between single- and dual-rest ^{201}Tl was considered to be high.

Case Example with Moore's Correction Method in Group 2B

Figure 10 shows representative ^{201}Tl myocardial polar maps of the relative regional uptake with a posteroinferior perfusion defect. The relative regional uptake in each segment of a dual ^{201}Tl image with Moore's correction method was closer to that of a single ^{201}Tl image than a dual ^{201}Tl image without correction.

DISCUSSION

In this study, we examined the feasibility of simultaneous stress ^{99m}Tc-sestamibi/rest ^{201}Tl dual-isotope myocardial perfusion SPECT in the detection of CAD. Quantitative assessment of the degree of correlation between single- and dual-isotope SPECT images demonstrated that Moore's crosstalk correction method is suitable for simultaneous dual-isotope SPECT. Simultaneous stress ^{99m}Tc-sestamibi/rest ^{201}Tl dual-isotope myocardial perfusion SPECT is an accurate method for the detection of CAD and the assessment of defect reversibility. Consequently, simultaneous stress ^{99m}Tc-sestamibi/rest ^{201}Tl dual-isotope myocardial perfusion SPECT with Moore's correction method appears to be an acceptable approach in clinical use.

Estimation of ^{201}Tl Crosstalk into the Dual-Stress ^{99m}Tc-Sestamibi Energy Windows

The relative regional uptake of single-stress ^{99m}Tc-sestamibi SPECT correlated well with that of dual-stress ^{99m}Tc-sestamibi SPECT, with a regression equation close to the identical line and a small 95% confidence interval for the mean value of estimated dual-stress ^{99m}Tc-sestamibi SPECT, and there was no difference in the relative regional uptake between single- and dual-stress ^{99m}Tc-sestamibi SPECT. These results suggest that dual-stress ^{99m}Tc-sestamibi SPECT images are similar to single-stress ^{99m}Tc-sestamibi SPECT images, and crosstalk correction is successful in eliminating ^{201}Tl contamination into the dual-stress ^{99m}Tc-sestamibi energy window. However, it was reported previously that the ^{99m}Tc-sestamibi photopeak image is only minimally affected

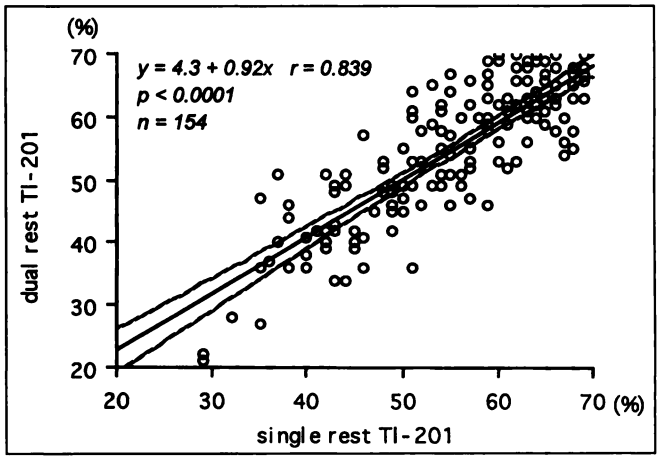

FIGURE 7. Correlation between relative regional uptake of ^{201}Tl obtained by single SPECT and by dual SPECT in segments with relative regional uptake values of single- and dual-rest ^{201}Tl ≤70%. Solid line represents regression line. Dotted curves represent 95% confidence interval for mean value of estimated dual-isotope SPECT ($y = 4.3 + 0.92x \pm 0.3\sqrt{100.9 + [x - 55.1]^2}$).

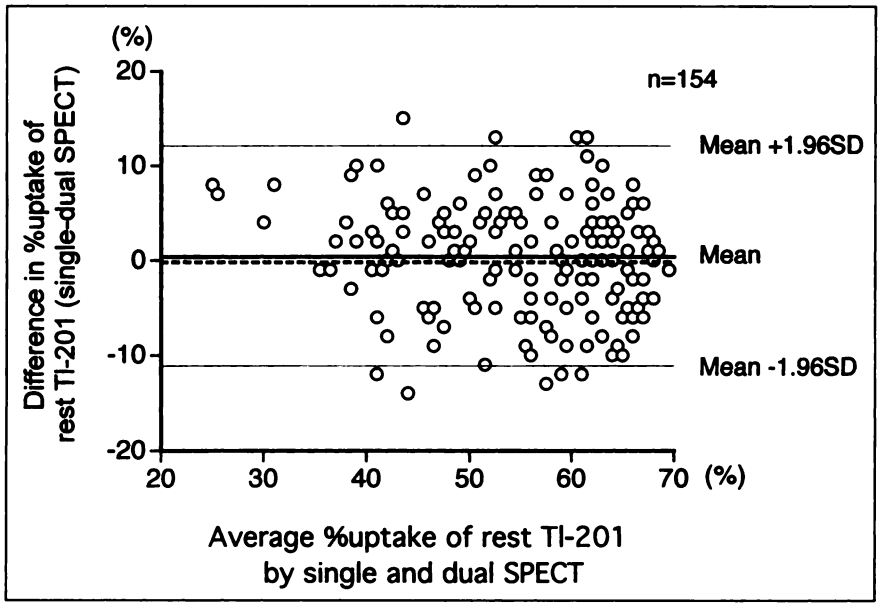

FIGURE 8. Difference in relative regional uptake values between single- and dual-rest ^{201}Tl SPECT plotted against their mean, with 95% confidence limits. Dotted line = mean ± 1.96 SD.

by the presence of ^{201}Tl photons because of their much lower abundance (*7,8*). Therefore, under typical clinical conditions with a high ^{99m}Tc-to-^{201}Tl ratio, the value of this correction may be negligible.

Estimation of ^{99m}Tc-Sestamibi Crosstalk into the Dual-Rest ^{201}Tl Energy Windows

Because of the higher energy of the ^{99m}Tc photons and the higher dose of ^{99m}Tc-sestamibi used, compared with that of ^{201}Tl, ^{99m}Tc-sestamibi crosstalk into dual-rest ^{201}Tl images has the potential to obscure ^{201}Tl defects without correction.

dual rest Tl-201

single rest Tl-201	21-30	31-40	41-50	51-60	61-70
21-30	2	0	0	0	0
31-40	2	6	4	1	0
41-50	0	7	21	6	0
51-60	0	1	8	23	17
61-70	0	0	0	15	41

FIGURE 9. Comparison of relative regional uptake value agreement between single- and dual-rest ^{201}Tl SPECT. Relative regional uptake values in range of 21%–70% were divided into five ranks at intervals of 10%.

Kiat et al. (*9*) reported that ^{99m}Tc crosstalk into ^{201}Tl windows contributed 27% of the dual ^{201}Tl counts. On the other hand, Lowe et al. (*10*) used cardiac and thoracic phantoms to evaluate a simultaneous dual-isotope acquisition without correction for ^{99m}Tc contamination. They reported a 10% reduction in defect contrast in dual ^{201}Tl as a result of ^{99m}Tc crosstalk and suggested that these changes were minimal. However, several caveats were pointed out in an accompanying editorial, which questioned whether the conclusions of the authors could be generalized to include larger attenuators and more realistic distributions of radiopharmaceutical uptake (*11*). Moore et al. (*12*) and Yang et al. (*13*) have reported simultaneous dual-isotope techniques for cardiac studies that make use of a third energy window to estimate the ^{99m}Tc scatter to be subtracted from the ^{201}Tl windows. To estimate as accurately as possible the spatial distribution of ^{99m}Tc scatter in the ^{201}Tl windows, the scatter window should be set as low in energy as possible without overlapping any of the ^{201}Tl x-rays. In addition, the scatter window should be wide enough to record sufficient counts to obtain a relatively low-noise estimate of the contamination. Therefore, Moore et al. (*6*) selected for this study the energy windows shown in Figure 3. Furthermore, by using a Monte Carlo program that simulates all details of photon transport, they demonstrated that lead x-rays produced in the collimator by photons with energy ≥ 88 keV also may contribute significantly to contamination in the ^{201}Tl windows. The spatial distribution of the ^{99m}Tc scattered photons differs from that of the lead x-rays. Thus, they modified their correction technique so that, at each projection angle, the contaminant image to be subtracted from the image in the ^{201}Tl windows was estimated as a linear combination of a scatter-window (90–110 keV) image (*5*).

In this study, the relative regional uptake of single-rest ^{201}Tl SPECT correlated well with that of dual-rest ^{201}Tl

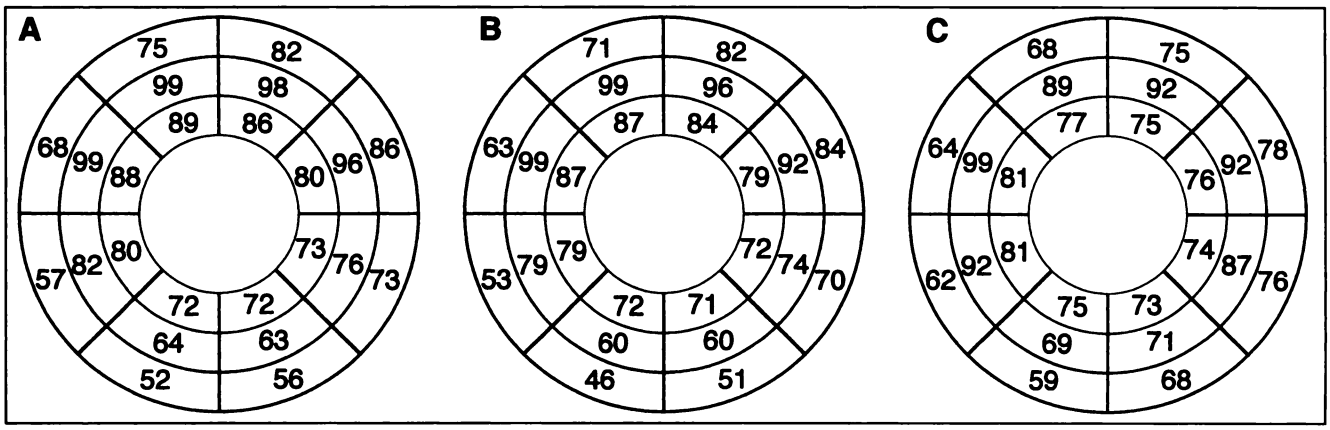

FIGURE 10. Example of ^{201}Tl myocardial polar map of relative regional uptake in single ^{201}Tl image (A) and dual ^{201}Tl image with Moore's correction method (B) and without correction (C) of group 2B patient with posteroinferior perfusion defect.

SPECT, with a regression equation close to the identical line and a small 95% confidence interval for the mean value of estimated dual-rest ^{201}Tl SPECT, and there was no difference in the relative regional uptake between single- and dual-rest ^{201}Tl SPECT. Furthermore, in the low ^{201}Tl uptake SPECT segments, the difference in the relative regional uptake values between single- and dual-rest ^{201}Tl SPECT against their mean using Bland-Altman analysis was not significant, and the concordance of the relative regional uptake between single- and dual-rest ^{201}Tl SPECT using the kappa statistic was high. The correction for the crosstalk of ^{99m}Tc into the ^{201}Tl windows in the infarcted area is most important. These results suggest that dual-rest ^{201}Tl SPECT images are similar to single-rest ^{201}Tl SPECT images. In addition, the dual-SPECT acquisitions for the patients in group 2B were obtained 30 min after methoxyisobutyl isonitrile (MIBI) injection, when the degree of washout of MIBI from the liver was still low. Accordingly, we were really testing the accuracy of correction for spilldown of ^{99m}Tc into the ^{201}Tl window under more difficult imaging conditions than would be expected for an actual clinical study, which means that this protocol provided a quite rigorous test of the accuracy of correction. Therefore, Moore's correction method for the ^{99m}Tc-induced contamination into the dual-rest ^{201}Tl appears acceptable for patient studies.

Sensitivity, Specificity and Accuracy for Coronary Artery Disease in Simultaneous Stress ^{99m}Tc-Sestamibi/Rest ^{201}Tl Dual-Isotope Myocardial Perfusion SPECT

In patient population studies, high sensitivity, specificity and accuracy were observed. In addition, although we excluded patients with previous myocardial infarction from the analysis of sensitivity for overall detection of CAD to avoid overestimation of test sensitivity, the sensitivity, specificity and accuracy were also high. A few patients with mild CAD were not identified by dual-isotope SPECT. The sensitivity of dual-isotope SPECT observed in this study is similar to that of SPECT studies using ^{201}Tl or ^{99m}Tc-sestamibi alone (*14,15*). The high accuracy in this study may be explained by the superior image quality obtained with stress ^{99m}Tc-sestamibi studies, which may have the effect of reducing artifactual defects (*16*).

Defect Reversibility

In this study, defect reversibility patterns on a territorial basis between patients with and without previous myocardial infarction were compared. Irreversible defects were infrequent in the patients without previous infarct, occurring in only 3 (11%) of 28 of the territories with stress defects. Conversely, in the patients with previous myocardial infarction, irreversible defects were significantly more common, occurring in 21 (95%) of 22 of the territories with stress defects. A significant difference ($P < 0.0001$) also was noted between patients with and without previous infarct with respect to the defect reversibility pattern when analyzed on a patient basis. These findings support the validity of simultaneous dual-isotope SPECT as performed in this study for the assessment of defect reversibility patterns. The clinical validity of the substitution of a rest ^{201}Tl for a rest ^{99m}Tc-sestamibi study is supported by the concordance of quantitatively assessed rest ^{201}Tl and rest ^{99m}Tc-sestamibi SPECT defects previously reported (*17*).

Potential Advantages and Disadvantages of Simultaneous Dual-Isotope SPECT

The simultaneous acquisition rest ^{201}Tl/stress ^{99m}Tc-sestamibi dual-isotope SPECT approach offers many advantages over currently available imaging techniques. Typically, an entire study takes only 90 min. This is 2.5–3.5 times faster than standard stress-redistribution ^{201}Tl or rest/stress ^{99m}Tc-sestamibi protocols, resulting in greater patient convenience and more rapid reporting. Also, critical to the widespread application of SPECT, which is frequently limited by available camera time, the simultaneous dual-imaging approach would optimize resource use by halving camera usage time compared with conventional SPECT protocols, thus potentially doubling throughput with existing equipment and personnel. Furthermore, when rest and stress studies are acquired simultaneously, many sources of error associated with the standard separate rest/stress acquisition

protocol can be eliminated or artifacts more readily identified as such. These include artifactual defects occurring as a result of patient motion during the rest or the stress study alone, shifting breast or other soft-tissue attenuation, changes in patient positioning between the two acquisitions and imprecise selection of appropriate slices or reorientation angles for comparison of rest and stress images.

Because two radioisotopes of differing energy are used in the dual-isotope approach, differences in defect resolution may be introduced (*1*). It is conceivable that irreversible defects identified by rest/stress ^{99m}Tc-sestamibi imaging might erroneously be identified as reversible by rest ^{201}Tl/stress ^{99m}Tc-sestamibi dual-isotope imaging. Also, there are differences in attenuation and scatter between ^{201}Tl and ^{99m}Tc-sestamibi, potentially resulting in the appearance of reverse redistribution of defects that are truly fixed and a fixed appearance of defects that are mildly reversible. Another consideration for dual-isotope imaging is the considerable variation of tracer distribution concentration extrinsic to the heart between ^{201}Tl and ^{99m}Tc-sestamibi. For ^{201}Tl, liver activity is minimal in stress images but greater in resting studies. For exercise or pharmacologic stress ^{99m}Tc-sestamibi studies, the amount of liver activity varies depending on the injection-to-imaging interval. Bowel tracer concentration may be considerable and may be two or three times greater than that in the myocardium. If ^{99m}Tc-sestamibi bowel activity scatters into the ^{201}Tl photopeak, an inferior ^{99m}Tc-sestamibi stress defect might appear reversible in the ^{201}Tl rest study.

Study Limitations

The dual-isotope method needs to be compared with standard techniques using either ^{201}Tl or ^{99m}Tc-sestamibi alone conducted sequentially in the same subjects. This would assess both comparative accuracy in identifying defects consistent with coronary stenosis as well as the protocol's ability to identify these defects as fixed or reversible in the same regions as the single-agent protocol.

This study used visual interpretation for analysis of the SPECT images. Visual interpretation introduced a potential source of variability. However, this was circumvented by the use of consensus reading by observers who were blinded to clinical history and outcome (*18*).

Furthermore, Moore et al. (*19*) showed that the optimal scaling parameters for the dual-isotope correction depend on the size of the patient. Although this correction was not used in this study, this may be a small effect that is approximately linear with patient size, because the distribution of the size or weight of patients in Japan is not as wide as that of patients in the U.S. In the future, perhaps a small correction for patient weight or size may be used to provide a refinement to the dual-isotope correction.

CONCLUSION

We evaluated the effectiveness of simultaneous acquisition rest ^{201}Tl/stress ^{99m}Tc-sestamibi dual-isotope myocardial perfusion SPECT with Moore's correction method and demonstrated that the sensitivities and specificities for CAD detection are similar to those in published studies with ^{201}Tl or ^{99m}Tc-sestamibi alone. This method has several advantages compared with standard ^{201}Tl or ^{99m}Tc-sestamibi protocols and is one of the current procedures of choice for performing same-day stress myocardial perfusion and myocardial viability SPECT studies.

ACKNOWLEDGMENT

This study was presented at the 44th Annual Meeting of the Society of Nuclear Medicine, San Antonio, TX, 1997.

REFERENCES

1. Berman DS, Kiat H, Friedman JD, et al. Separate acquisition rest thallium-201/stress technetium-99m sestamibi dual-isotope myocardial perfusion SPECT: a clinical validation study. *J Am Coll Cardiol.* 1993;22:1455–1464.
2. Matzer L, Kiat H, Wang FP, et al. Pharmacologic stress dual-isotope myocardial perfusion single-photon emission computed tomography. *Am Heart J.* 1994;128:1067–1076.
3. Heo J, Wolmer I, Kegel J, et al. Separate dual-isotope SPECT imaging with thallium-201 and technetium-99m-sestamibi. *J Nucl Med.* 1994;35:549–553.
4. Weinmann P, Foult J, Le Guludec D, et al. Dual-isotope myocardial imaging: feasibility, advantages and limitations. Preliminary report on 231 consecutive patients. *Eur J Nucl Med.* 1994;21:212–215.
5. Moore SC, English RJ, Syravanh C, et al. Simultaneous Tc-99m/Tl-201 imaging using energy-based estimation of the spatial distributions of contaminant photons. *IEEE Trans Nucl Sci.* 1995;42:1189–1195.
6. Moore SC, Zimmerman RE, Chan KH, et al. Experimental and Monte Carlo characterization of spectral and spatial distributions of lead x-rays [abstract]. *J Nucl Med.* 1994;35:61P.
7. Kiat H, Germano G, Van Train K, et al. Quantitative assessment of photon spillover in simultaneous rest ^{201}Tl/stress ^{99m}Tc sestamibi dual isotope myocardial perfusion SPECT [abstract]. *J Nucl Med.* 1992;33:854P.
8. Matzer L, Kiat H, Chen M, et al. Comparison of separate acquisition dual isotope SPECT including late redistribution imaging with rest/stress Tc-sestamibi SPECT for rest defect size and reversibility pattern [abstract]. *Circulation.* 1992;86:I-505.
9. Kiat H, Germano G, Friedman J, et al. Comparative feasibility of separate or simultaneous rest thallium-201/stress technetium-99m-sestamibi dual-isotope myocardial perfusion SPECT. *J Nucl Med.* 1994;35:542–548.
10. Lowe VJ, Greer KL, Hanson MW, Jaszczak RJ, Coleman RE. Cardiac phantom evaluation of simultaneously acquired dual-isotope rest thallium-201/stress technetium-99m dual-isotope cardiac SPECT images. *J Nucl Med.* 1993;34:1998–2006.
11. DePuey EG. Simultaneous thallium-201/technetium-99m dual-isotope cardiac SPECT: ready for prime time? [editorial]. *J Nucl Med.* 1993;34:2006–2008.
12. Moore SC, Syravanh C, Tow DE. Simultaneous SPECT imaging of Tl-201 and Tc-99m using four energy windows [abstract]. *J Nucl Med.* 1993;34:188P.
13. Yang DC, Ragasa E, Gould L, et al. Radionuclide simultaneous dual-isotope stress myocardial perfusion study using the "three window technique." *Clin Nucl Med.* 1993;18:852–857.
14. Leppo JA, DePuey EG, Johnson LL. A review of cardiac imaging with sestamibi and teboroxime. *J Nucl Med.* 1991;32:2012–2022.
15. Beller GA. Current status of nuclear cardiology techniques. *Curr Probl Cardiol.* 1991;16:451–535.
16. Berman DS, Kiat H, Maddahi J. The new 99m-Tc myocardial perfusion imaging agents: 99m-Tc sestamibi and 99m-Tc teboroxime. *Circulation.* 1991;84:17–21.
17. Maublant JC, Marcaggi X, Lusson JR, et al. Comparison between thallium-201 and technetium-99m methoxyisobutyl isonitrile defect size in single-photon emission computed tomography at rest, exercise and redistribution in coronary artery disease. *Am J Cardiol.* 1992;69:183–187.
18. Atwood JE, Jensen D, Froelicher V, et al. Agreement in human interpretation of analog thallium myocardial perfusion images. *Circulation.* 1981;64:601–609.
19. Moore SC, McIlvain TR, Kijewski MF. Compensation for Tc-99m contamination of Tl-201 images in simultaneous dual-isotope SPECT: effects of size of scattering medium. *IEEE Trans Med Imaging.* 1995;(suppl):207–211.